Nuclear Modification of Transverse Momentum Dependent Parton Distribution Functions by a Global QCD Analysis

Mishary Alrashed,[1,*] Daniele Anderle,[2,3,1,†] Zhong-Bo Kang,[1,4,5,‡] John Terry,[1,4,‖] and Hongxi Xing[2,3,§]

[1]*Department of Physics and Astronomy, University of California, Los Angeles, California 90095, USA*
[2]*Guangdong Provincial Key Laboratory of Nuclear Science, Institute of Quantum Matter, South China Normal University, Guangzhou 510006, China*
[3]*Guangdong-Hong Kong Joint Laboratory of Quantum Matter, Southern Nuclear Science Computing Center, South China Normal University, Guangzhou 510006, China*
[4]*Mani L. Bhaumik Institute for Theoretical Physics, University of California, Los Angeles, California 90095, USA*
[5]*Center for Frontiers in Nuclear Science, Stony Brook University, Stony Brook, New York 11794, USA*

(Received 11 August 2021; revised 13 July 2022; accepted 17 November 2022; published 7 December 2022)

We perform the first simultaneous global QCD extraction of the transverse momentum dependent (TMD) parton distribution functions and the TMD fragmentation functions in nuclei. We have considered the world set of data from semi-inclusive electron-nucleus deep inelastic scattering and Drell-Yan dilepton production. In total, this data set consists of 90 data points from HERMES, Fermilab, RHIC, and LHC. Working at next-to-leading order and next-to-next-to-leading logarithmic accuracy, we achieve a $\chi^2/\text{d.o.f.} = 1.196$. In this analysis, we perform the first extraction of nuclear modified TMDs and compare these to those in free nucleons. We also make predictions for the ongoing JLab 12 GeV program and future electron-ion collider measurements.

DOI: 10.1103/PhysRevLett.129.242001

Introduction.—In recent years, quantum 3D imaging of the nucleon has become one of the hottest research topics in nuclear physics [1]. Such information is encoded in the transverse momentum dependent parton distribution functions (TMDPDFs) and significant progress has been made in extracting TMDPDFs for free nucleons from experimental data [2–7]. On the other hand, the corresponding 3D imaging of a heavy nucleus is still at the primitive stage. Identifying the partonic structure of quarks and gluons in nuclei has remained one of the most important challenges confronting the nuclear physics community since the pioneering European Muon Collaboration (EMC) measurements in 1980s [8], and has been regarded as one of the major goals in future facilities of electron-ion colliders (EIC) [1,9,10]. Besides characterizing the nontrivial phenomena of nuclear modification of parton distribution inside bound nucleons and the associated QCD dynamics, an accurate determination of such initial state nuclear effect is mandatory for providing precise benchmark information in searching for the signal of quark-gluon plasma created in heavy-ion collisions [11].

Tremendous effort has been devoted to exploring the one-dimensional collinear nuclear parton distribution functions (nPDFs) [12]. Because of their nonperturbative nature, nPDFs have to be extracted through global analyses of relevant world data within the collinear factorization formalism [13]. Significant progress has been made [14–25], and recently charged current interactions have been used for flavor tagging, see for instance, EPPS16 [21], nCTEQ15 [26], nNNPDF [27]. Although there are theoretical models such as parton branching [28], multiple scattering in either intermediate Bjorken-x [29,30] or small-x saturation region [31], there remains no effort regarding the global extraction of the nuclear TMDPDFs (nTMDPDFs).

As demonstrated in both the generalized high-twist factorization formalism [32] and the dipole model [33,34], QCD multiple scattering in nuclei is responsible for the difference between TMDPDFs in bound and free nucleons. Such scattering leads to the transverse momentum broadening effect, manifested as the nuclear modification of the TMDPDFs within TMD factorization [35]. As such, while nTMDPDFs represent the 3D partonic imaging of nuclei, they are also crucial for understanding the QCD dynamics of multiple scattering in the nuclear medium. The accurate determination of nTMDPDFs is therefore one of the important objectives of the future EICs. Among the major goals of EICs, hadronization in the medium is also of particular interest, which has been investigated experimentally such as in HERMES [36]. Such information is usually

described by the nuclear-modified fragmentation functions (nFFs) involved in the same collinear factorization as that in vacuum [37,38]. However, how the hadronization is influenced by medium in three-dimensional momentum space, i.e., nuclear modified TMDFFs (nTMDFFs), has never been explored.

The determination of nTMDPDFs and nTMDFFs (collectively called nTMDs) relies on the corresponding TMD factorization [35] for physical observables that involve two distinct scales, which are required to guarantee both the applicability of pQCD and the sensitivity to the parton's transverse motion. Two well-known observables are the transverse momentum distribution of semi-inclusive hadrons in lepton-nucleus deep inelastic scattering (SIDIS) and of dilepton in Drell-Yan (DY) processes in proton-nucleus (pA) collisions. They have been measured by HERMES [36], JLab [39–41], Fermilab [42,43], RHIC [44], and the LHC [45,46], and will be further measured at the future EIC [1,9,10] with unprecedented precision.

In this Letter, we perform the first simultaneous QCD global analysis for the unpolarized nTMDPDFs and the unpolarized pion nTMDFFs using the world data from SIDIS and DY processes with nuclei. From our global analysis at next-to-leading order (NLO) and next-to-next-to-leading logarithmic (NNLL) accuracy, we perform the first-ever extraction of TMDs in bound nucleons.

TMD factorization formalism.—To perform global analysis, we select SIDIS and DY processes since TMD factorization [35] is well established for them. For ep SIDIS, $e(l)+p(P)\to e(l')+h(P_h)+X$, the cross section at small hadron transverse momentum $P_{h\perp}\ll Q$ is given by

$$\frac{d\sigma^p}{d\mathcal{PS}}=\sigma_0^{\rm DIS}H^{\rm DIS}(Q,\mu)\sum_q e_q^2\int_0^\infty\frac{bdb}{2\pi}J_0\left(\frac{bP_{h\perp}}{z}\right)\times f_{q/p}(x,b;\mu,\zeta_1)D_{h/q}(z,b;\mu,\zeta_2),\quad(1)$$

where, as in the standard TMD factorization, the result is written in the coordinate b space that is conjugate to $P_{h\perp}$. We have $d\mathcal{PS}=dxdQ^2dzd^2P_{h\perp}$ with $Q^2=-(l'-l)^2$, x and z the standard SIDIS kinematic variables, $\sigma_0^{\rm DIS}$ and $H^{\rm DIS}$ are the Born cross section and the hard function. $f_{q/p}$ is the quark TMDPDF inside a proton while $D_{h/q}$ denotes the TMDFF for $q\to h$, with μ and ζ representing the renormalization and rapidity scales. For the remainder of this Letter, we take $\mu=\sqrt{\zeta_1}=\sqrt{\zeta_2}=Q$ and replace their explicit dependence with the single scale Q. Within the Collins-Soper-Sterman formalism [47], the evolved TMDs take the following form:

$$f_{q/p}(x,b;Q)=[C_{q\leftarrow i}\otimes f_{i/p}](x,\mu_{b_*})e^{-S_{\rm pert}-S_{\rm NP}^f},\quad(2)$$

$$D_{h/q}(z,b;Q)=\frac{1}{z^2}[\hat{C}_{i\leftarrow q}\otimes D_{h/i}](z,\mu_{b_*})e^{-S_{\rm pert}-S_{\rm NP}^D},\quad(3)$$

where $C_{q\leftarrow i}$ and $\hat{C}_{i\leftarrow q}$ are the Wilson coefficient functions, $\otimes$ denotes the convolution, and $f_{i/p}(x,\mu_{b_*})$ and $D_{h/i}(z,\mu_{b_*})$ are the corresponding collinear PDFs and FFs. Here, $\mu_{b_*}=2e^{-\gamma_E}/b_*$ with γ_E the Euler constant represents the natural scale for TMD evolution, while b_* is the standard prescription.

TMD evolution handles the evolution for both the longitudinal momentum fraction (x, z) and transverse component $P_{h\perp}$ (or b in the coordinate space). The collinear functions in Eqs. (2) and (3) control the x (z) evolution via the usual Dokshitzer-Gribov-Lipatov-Altarelli-Parisi (DGLAP) evolution equation. On the other hand, the perturbative ($S_{\rm pert}$) and nonperturbative ($S_{\rm NP}^{f,D}$) Sudakov factors depend on b and Q, which control the corresponding perturbative (small b) and nonperturbative (large b) evolution on the parton's transverse momentum and eventually resums logarithms in $ln(Q^2/P_{h\perp}^2)$ after the Fourier transform. While $S_{\rm pert}$ is perturbatively calculable, $S_{\rm NP}^{f,D}$ have to be obtained by fitting experimental data and take the following form:

$$S_{\rm NP}^f(b,Q)=g_2(b)\ln(\sqrt{Q}/\sqrt{Q_0})+g_qb^2,\quad(4)$$

$$S_{\rm NP}^D(z,b,Q)=g_2(b)\ln(\sqrt{Q}/\sqrt{Q_0})+g_hb^2/z^2,\quad(5)$$

where $g_2(b)$ parametrizes the large-b behavior of the Collins-Soper evolution kernel and is both universal and independent of the species of external hadrons. We set $g_2(b)=g_2\ln(b/b_*)$ as in [48,49]. On the other hand, g_q (g_h) represents the intrinsic transverse momentum of the TMDs at the initial scale Q_0. In a simple Gaussian model, one has $g_q\sim\langle k_\perp^2\rangle/4$ [50,51], likewise for g_h. The parameters g_2, g_q, and g_h in vacuum are all constrained in [48] with $Q_0=\sqrt{2.4}$ GeV.

For the DY process in pp collisions, $p(P_1)+p(P_2)\to\gamma^*/Z(q)+X$, the cross section in the TMD factorization region is given by

$$\frac{d\sigma^p}{d\mathcal{PS}}=\sigma_0^{\rm DY}H^{\rm DY}(Q,\mu)\mathcal{P}(\eta,p_\perp^{\ell\ell})\sum_q c_q(Q)\int_0^\infty\frac{bdb}{2\pi}\times J_0(bq_\perp)f_{\bar{q}/p}(x_1,b;Q)f_{q/p}(x_2,b;Q),\quad(6)$$

where $d\mathcal{PS}=dQ^2dyd^2q_\perp$ with Q, y, $q_\perp$ the invariant mass, rapidity, and transverse momentum of the vector boson, while $c_q(Q)$ denotes the quark coupling to the γ^*/Z [4]. The term $\mathcal{P}$ takes into account the kinematic cuts on the transverse momentum $p_\perp^{\ell\ell}$ and the rapidity η of the final state lepton pair [4,6,7].

In going from a proton to a nuclear target, we follow the same procedure [12,52] that is used for the nuclear collinear PDFs and FFs and make two assumptions. First, we assume that the TMD factorization takes exactly the same form as in Eq. (1), except that one replaces the TMDs by the

nTMDs. Second, we assume that the perturbative physics for nTMDs and TMDs is the same. Our global analysis will thus test the validity of these assumptions, as was done in the pioneering work of [14]. Using these assumptions, the perturbative TMD evolution as controlled by $S_{\rm pert}$, would remain intact while the Wilson coefficient functions are also unchanged. Correspondingly, we would replace collinear functions in Eqs. (2) and (3) by their nuclear versions. In other words, these collinear functions would be modified at an initial scale Q_0 and then evolved to the scale μ_{b_*} via the same DGLAP equation. Finally, we modify the nonperturbative Sudakov $S_{\rm NP}^{f,D}$ to account for the nuclear effects. In principle, both $g_2(b)$ and $g_{q,h}$ could be modified [53] due to the transverse momentum broadening in the nucleus. We assume $g_2(b)$ to be the same as that for the proton, and only replace $g_{q,h}$ by their nuclear version $g_{q,h}^A$. The $g_{q,h}^A$ parameters would represent the parton's transverse momentum width inside a nucleus, which in general would depend on nuclear size ($\propto A^{1/3}$), momentum fraction x (or z) and the hard scale Q [54,55], denoted as $g_q^A(x,Q)$ and $g_h^A(z,Q)$. In the small-x or gluon saturation region, they would represent the typical size of saturation scale Q_s^2 [34,56].

Global analysis.—Considering the limited data available, we take the known parameters for collinear nPDFs $f_{i/p}^A(x,Q_0)$ and nFFs $D_{h/i}^A(z,Q_0)$, and perform the fit to extract $g_q^A(x,Q)$ and $g_h^A(z,Q)$. With more data in the future, one can simultaneously fit nuclear collinear functions and transverse modification encoded in $g_{q,h}^A$. Specifically, we use the EPPS16 [21] parametrization for collinear nPDFs with CT14nlo [57] for the proton PDFs, and we take LIKEn21 collinear nFFs in [52] for a nuclear target with the DSS14 parametrization [58] for the vacuum FFs. We have also performed this analysis using nCTEQ15 [26] for nPDFs and found no change to our conclusion [59]. In the kinematic region probed by the current data, the x (or z) and Q dependence is rather mild, which allows us to use two constant parameters a_N and b_N in the fit:

$$g_q^A(x,Q) = g_q + a_N L, \qquad g_h^A(z,Q) = g_h + b_N L, \quad (7)$$

where $L = A^{1/3} - 1$. Such a modification is similar to the change of the saturation scale Q_s^2 in the nucleus [33,34]. Thus, within our global analysis below, we have introduced the fit parameters a_N and b_N, which characterize the nuclear broadening for the nTMDs. We note that more complicated parametrizations for g_q^A and g_h^A lead to unstable fits due to the limited number of experimental data [59].

For the data, we take SIDIS measurements from HERMES and DY data from Fermilab, RHIC, and the LHC. HERMES [36] measured the hadron multiplicity ratio $R_h^A = M_h^A/M_h^D$, where the superscript A denotes the nucleus while D denotes a deuteron. On the other hand, $M_h^A = 2\pi P_{h\perp}(d\sigma^A/d\mathcal{PS})/(d\sigma^A/dxdQ^2)$, with the numerator given by the nuclear version of Eq. (1). The denominator is the inclusive DIS cross section, for which we use the APFEL library [60] at NLO with the collinear nPDFs. The CMS and ATLAS Collaborations at the LHC directly measure the transverse momentum distribution for γ^*/Z production, and we use the arTeMiDe library [4] to account for the phase space reduction in $\mathcal{P}$. Finally, for Fermilab and RHIC, experimental measurements were performed for nuclear modification factor $R_{AB} = (d\sigma^A/d\mathcal{PS})/(d\sigma^B/d\mathcal{PS})$, with A (B) the heavy (lighter) nucleus.

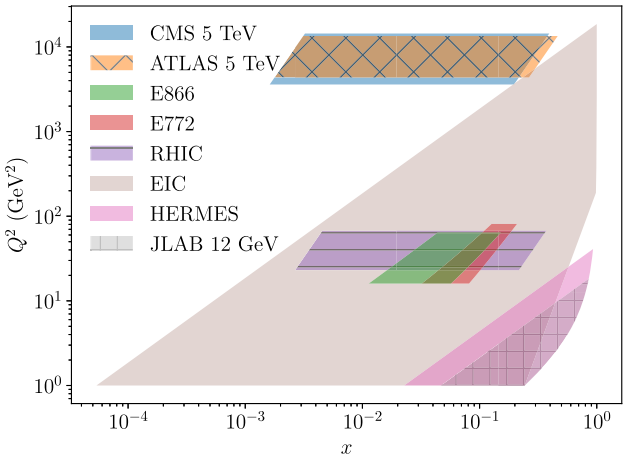

FIG. 1. Kinematic coverage for current experimental data and the projected coverage for JLab and the EIC.

To obtain the numerical values of a_N and b_N, we fit the experimental data using the MINUIT package [61]. Additionally, since the luminosity uncertainties at the LHC affect the normalization of these data, we consider a normalization factor $\mathcal{N}$ according to [21,58], see also Ref. [6]. In Fig. 1, we plot the kinematic coverage of the world data and that of the JLab and the future EIC. To select the HERMES data that is within the TMD region, we apply cuts $P_{h\perp}^2 < 0.3$ GeV^2 and $z < 0.7$. In order to avoid correlations between the experimental data at HERMES, we choose to fit only the $P_{h\perp}$ dependent data. Further, we note that in the LIKEn21 fit, these HERMES events have

TABLE I. The χ^2 of the central fit for each data set in our fit. (NA represents not applicable.).

Collaboration	Process	Baseline	Nuclei	$N_{\rm dat}$	χ^2
HERMES [36]	SIDIS (π)	D	Ne, Kr, Xe	27	16.3
RHIC [44]	DY	p	Au	4	2.0
E772 [42]	DY	D	C, Fe, W	16	20.1
E866 [43]	DY	Be	Fe, W	28	43.3
CMS [45]	γ^*/Z	NA	Pb	8	9.7
ATLAS [46]	γ^*/Z	NA	Pb	7	13.1
Total				90	105.2

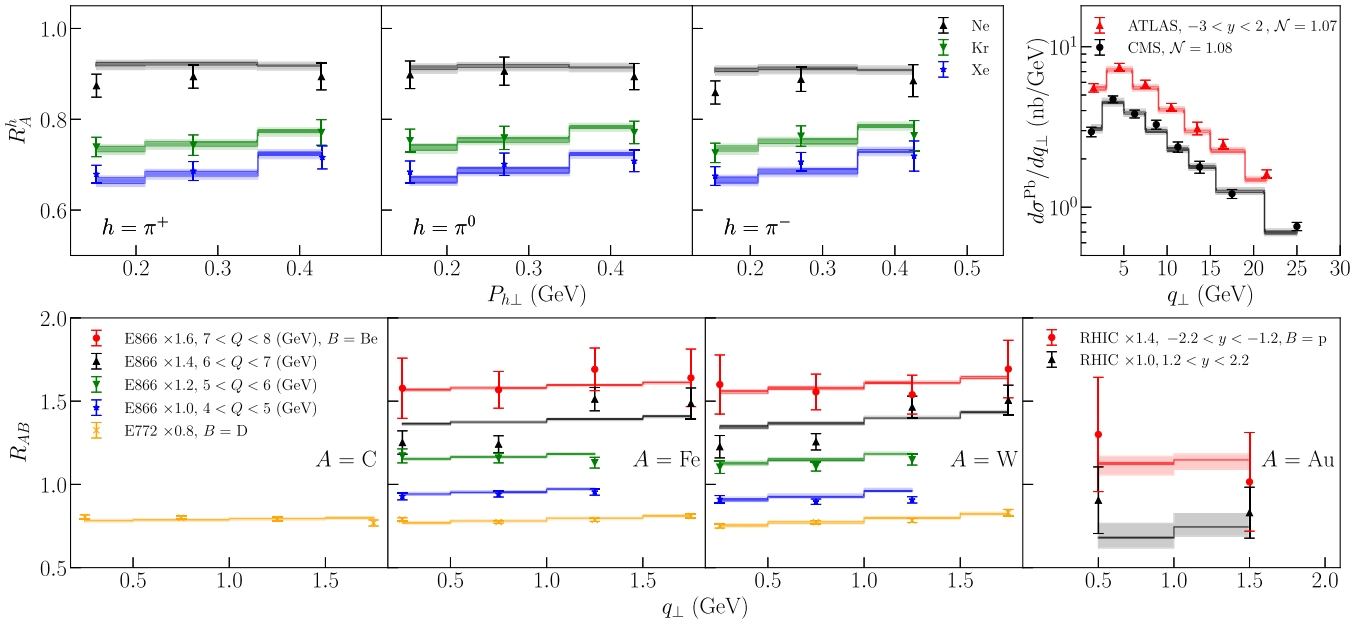

FIG. 2. Theoretical description of selected experimental data. The dark band represents the fit uncertainty while the light band represents the uncertainty from the nPDF and nFF.

already been taken into account. As a result, our analysis introduces some double counting of the HERMES events at small $P_{h\perp}$. For the DY data, we enforce the standard kinematic cut $q_\perp/Q < 0.3$. After performing these cuts, we are left with 90 points.

Results.—The global analysis of these parameters results in a χ^2/d.o.f. of 1.196 where we have $a_N = 0.016 \pm 0.003$ GeV^2 and $b_N = 0.0097 \pm 0.0007$ GeV^2. We note that the χ^2/d.o.f. with $a_N = b_N = 0$ being 6.183. Thus, the description of the experimental data when only considering nuclear modifications to the PDF and FF leads to a poor description of the data. The χ^2 for the central fit is provided in Table I for each data set. For the SIDIS data, we study only π production. The baseline column represents the lighter nuclei used in the SIDIS multiplicity ratio and the DY nuclear modification factor.

We consider two independent sources of uncertainty in the description of the experimental data. First, we consider the uncertainties associated with the fit by using the best fit of the collinear nPDFs and nFFs. To do this, we use the replica method in [62,63] with 200 replicas. Second, we consider the uncertainty associated with using the collinear nPDF and nFF and we use the prescription provided in [21] at 68%. In Figs. 2–4, the fit uncertainties are displayed as a dark band while uncertainties associated with the collinear distributions are displayed as lighter bands.

In Fig. 2, we plot the result of our fit against the experimental data. In the top row, we plot the comparison against the multiplicity ratio from HERMES [36] as a function of $P_{h\perp}$, and the DY $q_\perp$ distribution from the LHC (right column). Furthermore, for the LHC data [45,46], we have provided the $\mathcal{N}_i$ for each of the data sets. In the left three columns of the second row, we plot the comparison against the R_{AB} ratio for the E866 [43] and E772 [42] experiments. Finally, in the right column of this row, we plot the R_{AB} at RHIC [44]. We note that the size of the fit uncertainties is mainly driven by the E772 W data, which

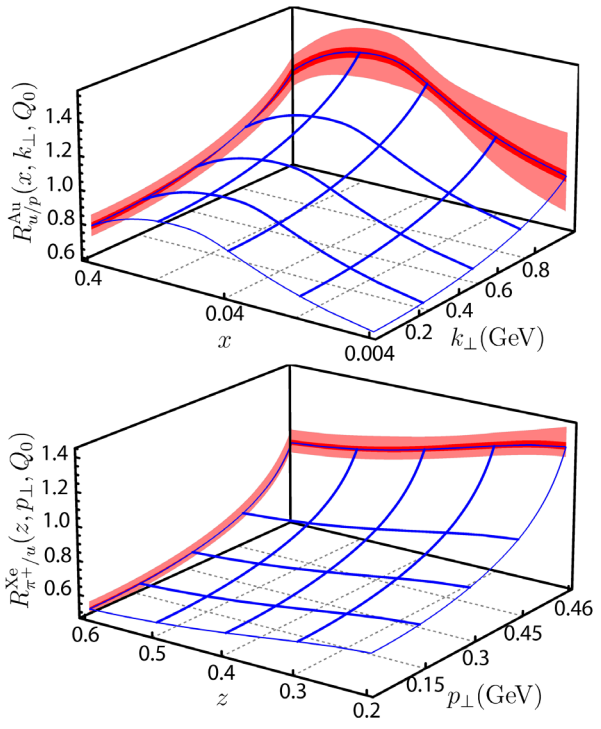

FIG. 3. The extracted nuclear ratio for the TMDPDF (top) and the TMDFF (bottom) at $Q_0 = \sqrt{2.4}$ GeV. The light and dark bands are the same as in Fig. 2.

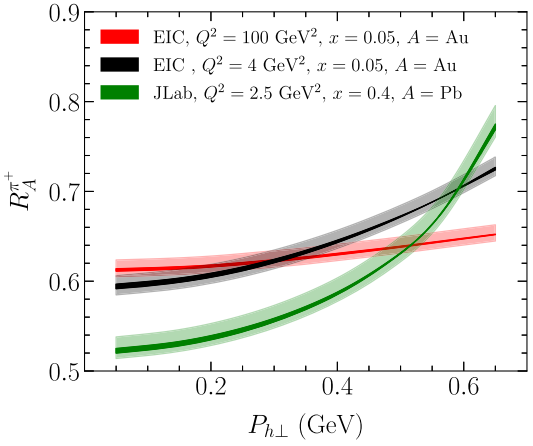

FIG. 4. Prediction for SIDIS π^+ production at the future EIC and JLab at $z = 0.4$. The light and dark bands are the same as in Fig. 2.

constrains our parametrization due to the high precision and large A value. Thus, while the size of our fit uncertainties are as large as the E772 W experimental errors, the fit uncertainties are smaller than the experimental uncertainties for many of the data [59].

In the top row of Fig. 3, we plot the ratio of the u-quark TMDPDF of a bound proton in a gold nucleus and that in a free proton as a function of x and $k_\perp$. Curves of constant $k_\perp$ are driven by the unfitted nPDFs which demonstrate shadowing, antishadowing, and the EMC effect. Curves of constant x are driven by the nonperturbative parametrization for the nuclear modification. Namely, since we obtain a positive a_N, the partons in nuclei are more broadly distributed in transverse momentum than in a proton. In the bottom row of this figure, we plot the ratio of the nTMDFF for $u \to \pi^+$ in a Xe. Once again the lines of constant $p_\perp$ are driven by the unfitted nFF while the lines of constant z are driven by the broadening parameter b_N, which we find to be positive in our analysis.

In Fig. 4, we plot our prediction for future JLab and EIC multiplicity ratio measurements as a function of $P_{h\perp}$ for π^+ at $z = 0.4$. For the EIC, we choose $x = 0.05$ and $Q^2 = 4$ GeV^2 (black) and $Q^2 = 100$ GeV^2 (red). For JLab, we choose $x = 0.4$ and $Q^2 = 2.5$ GeV^2 (green). We expect future measurements to provide a stringent constraint of nTMDs and to test the QCD evolution.

Summary.—We perform the first QCD global analysis of nuclear TMDs. For the processes with nuclei, assuming that TMD factorization and perturbative TMD evolution both take the same form as those in the vacuum, at the accuracy of NLO + NNLL we find that we can describe the global set of experimental data using a simple model which accounts for the nonperturbative TMD evolution. We demonstrate that both the TMDPDFs and TMDFFs in the presence of the nuclear medium have a broader distribution of transverse momentum. We expect that the framework we have developed will have a large impact on the interpretation of future experimental data at JLab, RHIC, LHC, and the future EICs, allowing us to perform quantum 3D imaging of the nucleus.

We thank Pia Zurita for providing us with the LIKEn21 parametrization. H. X. and D. P. A. are supported by the Guangdong Major Project of Basic and Applied Basic Research No. 2020B0301030008, the Key Project of Science and Technology of Guangzhou (Grant No. 2019050001), the National Natural Science Foundation of China under Grants No. 12022512, No. 12035007. D. P. A. is supported by the China Postdoctoral Science Foundation under Grant No. 2020M672668. M. A. is supported by the UCLA REU program and Ministry of Higher Education (MOHE) Merit Scholarship, Kuwait. Z. K. is supported by the National Science Foundation under Grant No. PHY-1945471. J. T. is supported by NSF Graduate Research Fellowship Program under Grant No. DGE-1650604 and UCLA Dissertation Year Fellowship. This work is supported within the framework of the TMD Topical Collaboration.

*misharyalrashed@g.ucla.edu
†dpa@m.scnu.edu.cn
‡Corresponding author.
zkang@ucla.edu
‖johndterry@physics.ucla.edu
§Corresponding author.
hxing@m.scnu.edu.cn

[1] A. Accardi *et al.*, Eur. Phys. J. A **52**, 268 (2016).
[2] M. Anselmino, M. Boglione, J. O. Gonzalez Hernandez, S. Melis, and A. Prokudin, J. High Energy Phys. 04 (2014) 005.
[3] A. Bacchetta, F. Delcarro, C. Pisano, M. Radici, and A. Signori, J. High Energy Phys. 06 (2017) 081; Erratum: 06 (2019) 051.
[4] I. Scimemi and A. Vladimirov, Eur. Phys. J. C **78**, 89 (2018).
[5] V. Bertone, I. Scimemi, and A. Vladimirov, J. High Energy Phys. 06 (2019) 028.
[6] I. Scimemi and A. Vladimirov, J. High Energy Phys. 06 (2020) 137.
[7] A. Bacchetta, V. Bertone, C. Bissolotti, G. Bozzi, F. Delcarro, F. Piacenza, and M. Radici, J. High Energy Phys. 07 (2020) 117.
[8] J. J. Aubert *et al.* (European Muon Collaboration), Phys. Lett. **123B**, 275 (1983).
[9] R. Abdul Khalek *et al.*, Nucl. Phys. **A1026**, 122447 (2022).
[10] D. P. Anderle *et al.*, Front. Phys. **16**, 64701 (2021).
[11] C. A. Salgado and J. P. Wessels, Annu. Rev. Nucl. Part. Sci. **66**, 449 (2016).
[12] J. J. Ethier and E. R. Nocera, Annu. Rev. Nucl. Part. Sci. **70**, 43 (2020).
[13] J. C. Collins, D. E. Soper, and G. F. Sterman, Adv. Ser. Dir. High Energy Phys. **5**, 1 (1989).

[14] K. J. Eskola, V. J. Kolhinen, and C. A. Salgado, Eur. Phys. J. C **9**, 61 (1999).
[15] D. de Florian and R. Sassot, Phys. Rev. D **69**, 074028 (2004).
[16] M. Hirai, S. Kumano, and T. H. Nagai, Phys. Rev. C **76**, 065207 (2007).
[17] K. J. Eskola, V. J. Kolhinen, H. Paukkunen, and C. A. Salgado, J. High Energy Phys. 05 (2007) 002.
[18] I. Schienbein, J. Y. Yu, K. Kovarik, C. Keppel, J. G. Morfin, F. I. Olness, and J. F. Owens, Phys. Rev. D **80**, 094004 (2009).
[19] S. Atashbar Tehrani, Phys. Rev. C **86**, 064301 (2012).
[20] H. Khanpour and S. Atashbar Tehrani, Phys. Rev. D **93**, 014026 (2016).
[21] K. J. Eskola, P. Paakkinen, H. Paukkunen, and C. A. Salgado, Eur. Phys. J. C **77**, 163 (2017).
[22] M. Walt, I. Helenius, and W. Vogelsang, Phys. Rev. D **100**, 096015 (2019).
[23] K. Kovarik *et al.*, Phys. Rev. D **93**, 085037 (2016).
[24] R. Abdul Khalek, J. J. Ethier, and J. Rojo (NNPDF Collaboration), Eur. Phys. J. C **79**, 471 (2019).
[25] R. Abdul Khalek, J. J. Ethier, J. Rojo, and G. van Weelden, J. High Energy Phys. 09 (2020) 183.
[26] K. Kovařík, A. Kusina, T. Ježo, D. Clark, C. Keppel, F. Lyonnet, J. Morfín, F. Olness, J. Owens, I. Schienbein *et al.*, Phys. Rev. D **93**, 085037 (2016).
[27] R. A. Khalek, J. J. Ethier, and J. Rojo, Eur. Phys. J. C **79**, 471 (2019).
[28] E. Blanco, A. van Hameren, H. Jung, A. Kusina, and K. Kutak, Phys. Rev. D **100**, 054023 (2019).
[29] A. Schäfer and J. Zhou, Phys. Rev. D **88**, 074012 (2013).
[30] Y.-Y. Zhang and X.-N. Wang, Phys. Rev. D **105**, 034015 (2022).
[31] Y. V. Kovchegov and M. D. Sievert, Nucl. Phys. **B903**, 164 (2016).
[32] Z.-t. Liang, X.-N. Wang, and J. Zhou, Phys. Rev. D **77**, 125010 (2008).
[33] A. H. Mueller, B. Wu, B.-W. Xiao, and F. Yuan, Phys. Lett. B **763**, 208 (2016).
[34] A. H. Mueller, B. Wu, B.-W. Xiao, and F. Yuan, Phys. Rev. D **95**, 034007 (2017).
[35] J. Collins, *Foundations of Perturbative QCD* (Cambridge University Press, Cambridge, England, 2013), Vol. 32.
[36] A. Airapetian *et al.* (HERMES Collaboration), Nucl. Phys. **B780**, 1 (2007).
[37] R. Sassot, M. Stratmann, and P. Zurita, Phys. Rev. D **81**, 054001 (2010).
[38] X.-f. Guo and X.-N. Wang, Phys. Rev. Lett. **85**, 3591 (2000).
[39] M. Arratia, Y. Furletova, T. J. Hobbs, F. Olness, and S. J. Sekula, Phys. Rev. D **103**, 074023 (2021).
[40] J. Dudek *et al.*, Eur. Phys. J. A **48**, 187 (2012).
[41] V. D. Burkert, in *CLAS 12 RICH Detector Workshop* (2008), arXiv:0810.4718.
[42] D. M. Alde, H. W. Baer, T. A. Carey, G. T. Garvey, A. Klein *et al.*, Phys. Rev. Lett. **64**, 2479 (1990).
[43] M. A. Vasilev, M. E. Beddo, C. N. Brown, T. A. Carey, T. H. Chang *et al.* (NuSea Collaboration), Phys. Rev. Lett. **83**, 2304 (1999).
[44] Y. H. Leung (PHENIX Collaboration), Proc. Sci., HardProbes 2018 (**2018**) 160.
[45] V. Khachatryan *et al.* (CMS Collaboration), Phys. Lett. B **759**, 36 (2016).
[46] G. Aad *et al.* (ATLAS Collaboration), Phys. Rev. C **92**, 044915 (2015).
[47] J. C. Collins, D. E. Soper, and G. F. Sterman, Nucl. Phys. **B250**, 199 (1985).
[48] M. G. Echevarria, Z.-B. Kang, and J. Terry, J. High Energy Phys. 01 (2021) 126.
[49] Z.-B. Kang, A. Prokudin, P. Sun, and F. Yuan, Phys. Rev. D **93**, 014009 (2016).
[50] S. M. Aybat and T. C. Rogers, Phys. Rev. D **83**, 114042 (2011).
[51] M. Anselmino, M. Boglione, and S. Melis, Phys. Rev. D **86**, 014028 (2012).
[52] P. Zurita, arXiv:2101.01088.
[53] Z.-B. Kang and J.-W. Qiu, Phys. Lett. B **721**, 277 (2013).
[54] Z.-B. Kang, E. Wang, X.-N. Wang, and H. Xing, Phys. Rev. Lett. **112**, 102001 (2014).
[55] P. Ru, Z.-B. Kang, E. Wang, H. Xing, and B.-W. Zhang, Phys. Rev. D **103**, L031901 (2021).
[56] F. Gelis, E. Iancu, J. Jalilian-Marian, and R. Venugopalan, Annu. Rev. Nucl. Part. Sci. **60**, 463 (2010).
[57] S. Dulat, T.-J. Hou, J. Gao, M. Guzzi, J. Huston, P. Nadolsky, J. Pumplin, C. Schmidt, D. Stump, and C. P. Yuan, Phys. Rev. D **93**, 033006 (2016).
[58] D. de Florian, R. Sassot, M. Epele, R. J. Hernández-Pinto, and M. Stratmann, Phys. Rev. D **91**, 014035 (2015).
[59] See Supplemental Material at http://link.aps.org/supplemental/10.1103/PhysRevLett.129.242001 for additional analyses in investigating possible biases from the choice of parametrization, the treatment of the uncertainties, as well as the choice of collinear nPDF and nFF sets.
[60] V. Bertone, S. Carrazza, and J. Rojo, Comput. Phys. Commun. **185**, 1647 (2014).
[61] F. James and M. Roos, Comput. Phys. Commun. **10**, 343 (1975).
[62] R. D. Ball, L. Del Debbio, S. Forte, A. Guffanti, J. I. Latorre, A. Piccione, J. Rojo, and M. Ubiali (NNPDF Collaboration), Nucl. Phys. **B809**, 1 (2009); **B816**, 293(E) (2009).
[63] A. Signori, A. Bacchetta, M. Radici, and G. Schnell, J. High Energy Phys. 11 (2013) 194.